Progressive Multi-Cracking of Fiber Composite Structures

S. Mohammadi[1], R. Rahmani Amlashi[1] and A. Asadollahi [1]*
[1]Dept. Of Civil Engineering, University of Tehran, Iran,
[1] Email: smoham@shafagh.ut.ac.ir (corresponding author)*

Abstract

A combined finite/discrete element model has been developed to study the damage mechanism of laminated composites. Interaction and coupling between in-plane cracks and interlaminar delamination has also been considered. An algorithm is provided for including tangential/frictional sliding within the penalty contact algorithm. The Hashin criterion has been adopted for modeling the composite anisotropic behaviour. The ability of the method for simulation of damage is assessed by comparing standard test cases available in the literature.

1. Introduction

Composites are used in a wide variety of applications, such as vehicles, sport equipments, aerospace industry, etc. Composite materials were developed because no single, homogeneous structural material could be found that had all desired attributes for a given application. They are attractive to design engineering because of their high strength-to-weight ratio, superior corrosion resistance, high fatigue strength etc.

One of the problems that must be investigated in the performance of composite materials, particularly in impact loading conditions, is "cracking " phenomenon. Experimental observations have shown that matrix cracks and delamination resulting from impact seem to appear concurrently, indicating the existence of a strong interaction between matrix cracking and delamination during impact. Figure (1) illustrates these failure modes and the coupling between them for a bending beam with an initial notch.

Recent developments of the discrete element method have opened a new approach to modeling this behaviour based on discontinuum mechanics. In constrant, most computational simulations have employed continuum based finite elements to evaluate the initiation and propagation of cracks in composites. In past, a simple criterion based on the comparison of normal stress to a maximum value was used. Later, more complex models were developed for different types of laminates. In early simulations, continuum elasticity was frequently used to formulate the governing equations [1]. The main disadvantage of those schemes was in their restriction to linear geometry of laminates [2,3]. The next step to a more rational model was achieved by development of contact interaction algorithm. Liu et al. [4] used a contact analysis for modeling the interface behaviour of laminate composite. Recently, Mohammadi et al. employed a contact algorithm and a Culomb friction law to study the progressive damage of composites [5].

Fracture mechanics concepts have been widely adopted in the development of crack propagation algorithms to model the extension of delamination [6,7]. Several criteria have been proposed to include the effect of individual or mixed modes of fracture. In some of recent researches, interface elements were used for simulation of progressive delamination. For example, Mi. et al. used these elements in conjunction with softening relationships between the stresses and the relative displacements [7].

In the present work, a combined finite/discrete element methodology is employed for modeling and controlling of cracking process. In the following, after reviewing the modeling procedure, the main formulations for failure analysis, finite element analysis and contact interaction will be discussed. Then remeshing procedure will be described which is used at the present work. Finally, the performance of the model will be assessed by some of the numerical results.

2. Modeling Procedure

At the present work, a combined finite/discrete method is employed for simulation of composites. Discrete elements are used for the segments with delamination possibility and the rest of the structure is discretized by a standard finite

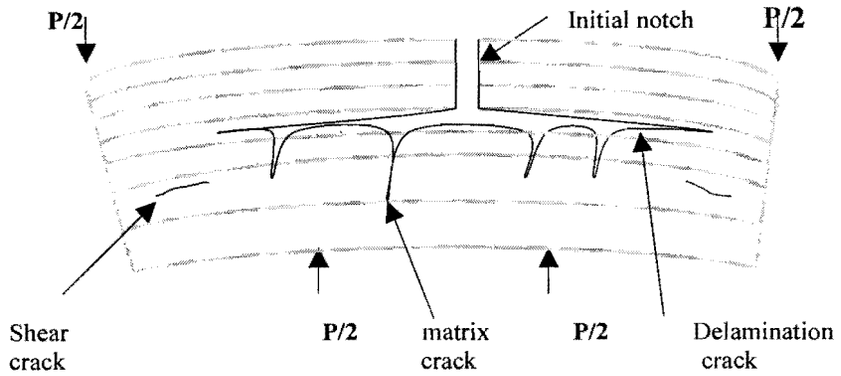

Fig.1 : Failure modes in a typical composite specimen

element mesh. For this purpose, similar plies are modeled by one discrete element and a finite element mesh is employed for modeling individual discrete elements. Interaction between finite and discrete elements are considered by a proper interface transition law, which prevents debonding under all stress conditions. The interlamiar behaviour of discrete elements is governed by bonding laws including contact and friction interactions for the post delamination phase. A combined mesh helps us to prevent unnecessary contact detection and interaction calculations.

In order to achieve an efficient simulation, an explicit dynamic analysis has been adopted. The model consists of three steps: a standard finite element analysis, a contact analysis and a failure analysis. The FE analysis is performed for calculating the stress and deformation of the composite laminates. The contact analysis adopts a penalty method for dealing with interface conditions of matrix cracks and delamination during impact loading. Finally, the failure analysis is proposed for predicting the occurrence of matrix cracking and for modeling delamination initiation and propagation.

2.1 Finite Element Analysis

A finite element formulation based on the weak form of the boundary value problem has been adopted. Let Ω represent the body of interest and Γ denote its boundary. In a standard fashion the boundary is assumed to consist of a part with prescribed displacement u_i, Γ_{ui} and a part with prescribed traction force fi^{surf}, $\Gamma_{\sigma i}$. In addition it is assumed that a part Γ_c may be in contact with another body. By denoting with

$$V: =\{\delta \mathbf{u}: \delta u_i = 0 \text{ on } \Gamma_{ui}\} \tag{1}$$

as the space of admissible variations, the variational form of the dynamic initial/boundary value problem ca be expressed as

$$W^{int}(\delta \mathbf{u}, \mathbf{u}) + M(\delta \mathbf{u}, \mathbf{u}) = W^{ext}(\delta \mathbf{u}) + W^{con}(\delta \mathbf{u}) \tag{2}$$

where

$$W^{int}(\delta \mathbf{u}, \mathbf{u}) = \int_{\Omega} \delta\varepsilon(\mathbf{u}) : \sigma(\mathbf{u})\, dv, \tag{3}$$

$$M(\delta \mathbf{u}, \mathbf{u}) = \int_{\Omega} \delta \mathbf{u} \cdot \rho \ddot{u}\, dv, \tag{4}$$

$$W^{ext}(\delta \mathbf{u}) = \int_{\Omega} \delta \mathbf{u} \cdot \mathbf{f}^{body}\, dv + \int_{\Gamma_\sigma} \delta \mathbf{u} \cdot \mathbf{f}^{surf}\, da, \tag{5}$$

$$W^{con}(\delta \mathbf{u}) = \int_{\Gamma_c} \delta \mathbf{g}(\mathbf{u}) \cdot \mathbf{f}^{con}\, da \tag{6}$$

denote, respectively, the virtual work of internal forces, the inertial forces contribution, the virtual work of external forces and the virtual work of contact forces. Here $\boldsymbol{\sigma}$ is the Cauchy stress tensor, $\boldsymbol{\varepsilon}$ is the strain tensor, $\mathbf{u}$ is the displacement vector, while $\mathbf{g}$ represents the contact gap vector.

2.2 Failure Analysis

A set of failure criteria was proposed for predicting damaged caused by different types of failure mechanisms [4]. The distinction between various modes of failure is very important since different failure mechanisms result in totally different types of damage growth and lead to different failure loads. The Hashin failure criterion, which can predict the fiber failure mode and the matrix mode of failure, is used to predict the lamina failure [8]. According to this criterion, failure can be defined by:

Tensile fiber mode $(\sigma_{11} > 0)$: $$(\frac{\sigma_{11}}{X_T})^2 + (\frac{\sigma_{11}}{S})^2 = 1 \quad (7)$$

Compressive fiber mode $(\sigma_{11} < 0)$: $$|\sigma_{11}| = X_C \quad (8)$$

Tensile matrix mode $(\sigma_{22} > 0)$: $$(\frac{\sigma_{22}}{Y_T})^2 + (\frac{\sigma_{12}}{S})^2 = 1 \quad (9)$$

Compressive matrix mode $(\sigma_{22} < 0)$: $$(\frac{\sigma_{22}}{2S_T})^2 + [(\frac{Y_C}{2S_T})^2 - 1]\frac{\sigma_{22}}{Y_C} + (\frac{\sigma_{12}}{S})^2 = 1 \quad (10)$$

where

X_C, X_T = longitudinal compressive and tensile strengths, respectively

Y_C, Y_T = transverse compressive and tensile strengths, respectively

S_T, S = longitudinal and transverse shear strengths, respectively

and σ_{11}, σ_{22}, and σ_{12} are the two longitudinal and tangential stresses, respectively.

Whenever the combined state of stresses satisfies the criterion, initial failure occurrs. The corresponding failure criterion indicates the initial mode of failure. Once the initial mode is predicted, another criterion should be introduced to simulate the growth of the local damage as the loading continues.

A softening material model according to [Figure (2)] is adopted where the tensile strength f_t, the "cracking strain" ε_t, and the "maximum strain" ε_u are defined as material properties. In the finite element simulations, the strain can exceed ε_u, but the equivalent stress will then be set to zero; that is the crack opening is complete. The region $\varepsilon_t < \varepsilon < \varepsilon_u$ represents the softening behaviour of the element.

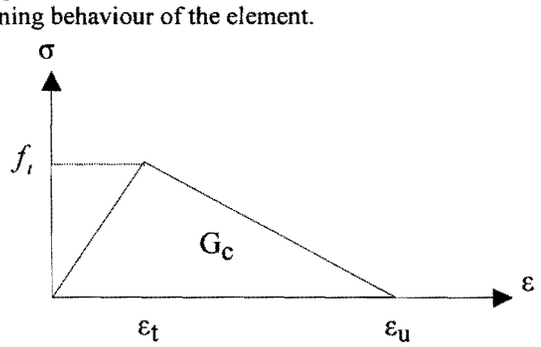

Fig. 2: Bilinear softening model

In relation to figure (2), the critical fracture energy G_c, is defined as the integral of the area under the softening branch of the stress-strain curve:

$$G_c = [0.5\, f_t\, (\varepsilon_u - \varepsilon_t)]\, l_c \quad (11)$$

where l_c is the localization bandwidth. In general, l_c is contained within one element and, as a close approximation it may be defined based on the area A, or the volume of the fractured element, V,

$$l_c = A^{0.5} \text{ for 2D} \qquad (12)$$
$$l_c = V^{1/3} \text{ for 3D}$$

The softening modulus is then defined as

$$E_P = \frac{f_t^2 l_c}{2G_C} \qquad (13)$$

The Hashin criterion cannot predict the crack direction correctly. A simple method is based on the assumption that the material cracks are only formed along or perpendicular to the fiber direction. Figure (3) illustrates this simple assumption for two dimensional problems.

Out of plane fibers. Inplane fibers.

Fig. 3 : Crack direction in composites

2.3 Contact Analysis

An algorithm is provided for including tangential stiffness and frictional sliding within the penalty contact algorithm for explicit analysis. The tangential force is defined as

$$f_t = \alpha_t g_t \qquad (14)$$

where g_t is the tangential component of the relative motion (gap) and α_t is the elastic tangential stiffness or penalty coefficient. The tangential gap is defined as

$$^{t+\Delta t}g_t = {}^{t}g_t + (^{t+\Delta t}\xi_c - {}^{t}\xi_c)\, {}^{t}l \qquad (15)$$

where the local coordinate system, ξ, so that $\xi \in [0,1]$, is used.

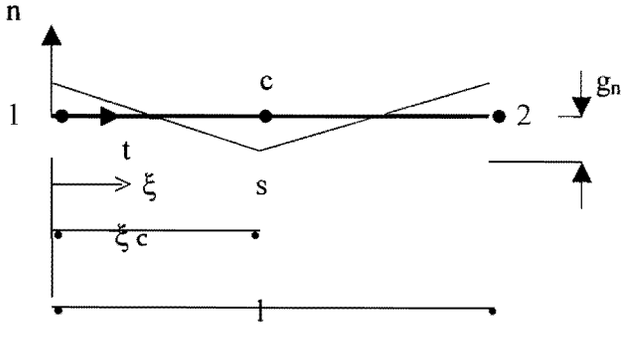

Fig. 4

and ξ_c is the local coordinates of the point c, defined by the normal projection of the contact point s onto the segment i.e:

$$\xi_c = (\mathbf{x_s}-\mathbf{x_1}).\mathbf{t}/l \tag{16}$$

where $\mathbf{x_s}, \mathbf{x_1}$ are the global coordinates of the points 1,s.

Simple Coulomb Friction

The simple classical Culomb friction law is employed to calculate friction forces. According to this assumption, there is no relative motion until the maximum allowable tangential friction force is reached. This behavior, can be formulated as

$$\begin{aligned} \Delta u_t &= 0 \quad \text{if} \quad |f_t| < \mu f_n \\ \Delta u_{t\neq} &0 \quad \text{if} \quad |f_t| = \mu f_n \end{aligned} \tag{17}$$

where Δu_t is the relative tangential displacement of two surfaces and μ is the friction coefficient. Once $\Delta u_{t\neq}0$, the tangential gap can be writen as

$$g_t = g_t^e + g_t^p \tag{18}$$

where g_t^e, g_t^p are the elastic and plastic tangential gaps. Using the flow rule, g_t^p is given as

$$\Delta g_t^p = \Delta\lambda \, \partial\Phi/\partial f_t \tag{19}$$

Where $\Delta\lambda$ is the constant coefficient of flow rule. For simple coulomb friction the yield function or slip condition is defined as

$$\Phi = |f_t| - \mu f_n \tag{20}$$

The stress update algorithm can be achieved by implementing the and following the standard plasticity procedures flow rule [as described in box (1)]

Box.1 - Stress update algorithm with coulomb friction slip

Compute tangential displacement

$$\Delta g_t = ({}^{t+\Delta t}\xi_c - {}^{t}\xi_c)\,{}^{t}l$$

Evaluate trial tangential stress

$$f_t^{trial} = {}^{t}f_t + \alpha_t \Delta g_t$$

Compute yield function for f_t^{trial}

$$\Phi^{trial} = \| \, {}^{t+\Delta t}f_t^{trial} \, \| - \mu f_n$$

f_n =constant

IF $\Phi^{trial} \leq 0$ (Elastic phase)

$${}^{t+\Delta t}f_t = f_t^{trial}$$

$$\Delta g_t^p = 0$$

ELSE (Perform correction for frictional slip)

$${}^{t+\Delta t}f_t = \mu \, {}^{t+\Delta t}f_n \, \text{sign}({}^{t+\Delta t}f_t^{trial})$$

$$\Delta\lambda = [\| \, {}^{t+\Delta t}f_t^{trial} \, \| - \mu \, {}^{t+\Delta t}f_n]$$

3. Remeshing Procedure

Material fracture may result in the creation of new discrete bodies, which are in contact and friction interaction with neighboring bodies. A special remeshing algorithm is adopted to maintain compatibility conditions in newly fractured regions.
The failure indicator and the crack direction for each individual element are evaluated within the material model routines. A weighted averaging scheme is then used to evaluate both the failure indicator and crack direction of each node. The next step is to geometrically simulate the crack and perform the necessary split, separation and the remeshing processes. Figure (5) represents the two dimensional remeshing algorithm which comprises four steps :

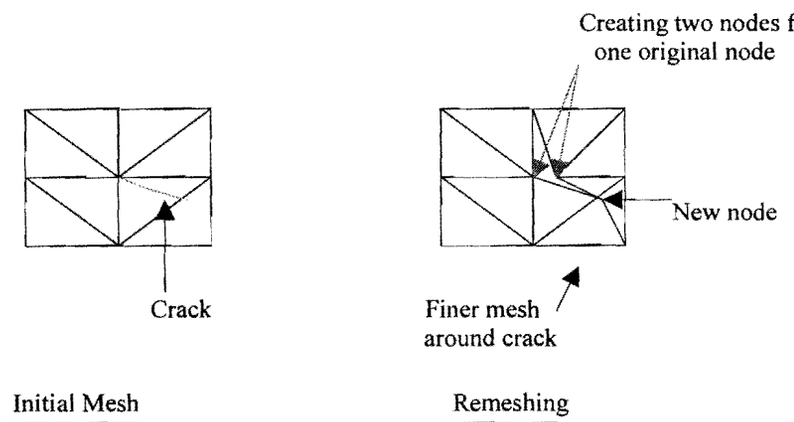

Fig. 5: Remeshing algorithm

splitting the element, separating the failed nodes, creating new remeshing nodes, and dividing uncracked elements to enforce compatibility at new nodes. Adopting this local remeshing algorithm will provide a relatively finer mesh in the fractured region and prevents the distortion of the elements in this region. Also in the crack adjacent, meshes became smaller, which improves the finite element approximation of the analysis [see figure (5)]. After remeshing, it is not required to reanalysis the whole model in each step. The stress state is transformed from parent to new elements. They are first extrapolated from the old element gauss points to the element nodes, and then they will be interpolated to the new element gauss points. Special attention has to be made to avoid violation of equilibrium equations at new gauss points.

4. Numerical Results

4.1 Impact Induced Delamination in a Composite Plate

A composite plate, clamped in its two opposite sides and free in the other two, impacted with a cylindrical nose steel impactor along its central line. The plate is 10 cm long and $[0_6/90_4/0_6]$ composite layup with a total thickness of 2.3 mm [figure (6)]. Material properties of the plate and impactor object are defined in table (1). Because of the symmetry, only half of the problem has been modeled and only the delamination of the plate is considered. A full fracture analysis of the plate with matrix cracking was performed in ref. [11] by using 33180 LST and 23773 cohesive triangle elements. The deformation and delamination patterns of the plate are shown in figures (7) and (8) at times 0.1ms, 0.6 ms, respectively. Displacement history of central point of the plate has been shown in figure 9.

The present simulation is performed with discrete elements, showing a great reduction in computational efforts, comparing to the modeling procedure undertaken by Geubelle et al. [11].

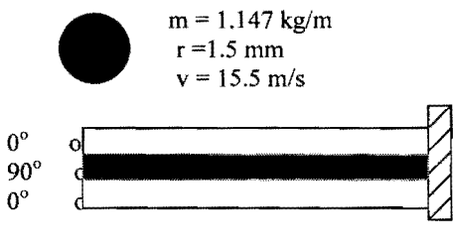

Fig 6: Geometry of composite impact problem

Table (1)- Material Properties of Composite Plate	
E_{xx}= 156 GPa	E_{yy}= 9.09 GPa
ν_{xy}=0.228	ν_{yz}=0.4
G_{IC}=147 J/m^2	G_{IIC}=526 J/m^2
ρ= 1540 kg/m^2	

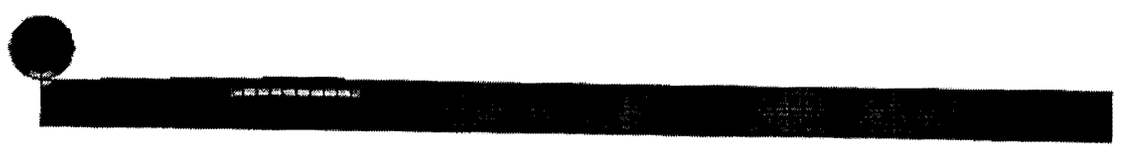

Fig.7: Delamination pattern at time 0.1 ms

Fig.8: Delamination pattern at time 0.6 ms

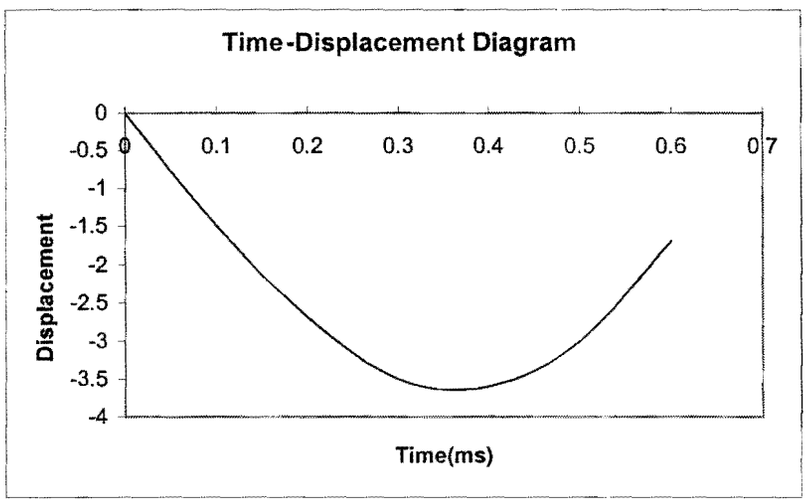

Fig.9: Displacement history of central point of the plate

4.2 Buckling Simulation of a Delaminated Composite Panel

A composite panel with an initial interlaminar crack is considered here to inspect its behavior under compressive loading as depicted in figure (10). The panel consists of $[0_{20}]$ layers. An initial interlaminar crack exists between the $0_4/0_{16}$ layers. The material properties are listed in Table (2). Normal and frictional contact interaction laws have been considered for delaminated layers, while mixed mode criteria have been adopted for the calculation of delamination propagation. The loading incrementally continues until the local and global buckling occur in 0_4 and 0_{16} layers, respectively. Figures (11), (12) and (13) show deformation configuration of the panel after local and global buckling. As shown in figures (14) and (15), local buckling commenced at load 1410 (lbf/in) and global buckling occurred at load 7130 (lbf/in). The same problem was modeled by Progini et al. [11]. The local and global loads where reported to be 1312 (lbf/in) and 7821 (lbf/in), respectively, showing a very good agreement with the present results.

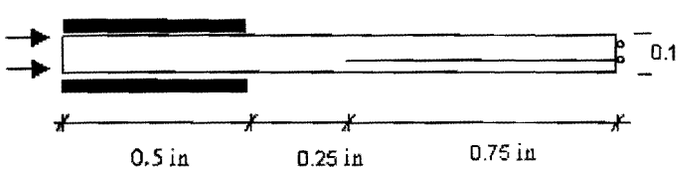

Fig.10: composite panel with an initial interlaminar crack

Table(2)- Material Properties of Composite Panel	
E_{xx}= 20200 ksi	E_{yy}=1410 ksi
E_{zz}=1410 ksi	G_{xy}=810 ksi
G_{yz}=546 ksi	v_{xy}=0.29
v_{xz}=0.29	v_{yz}=0.29
X_T=220 ksi	X_C=231 ksi
Y_T=6.46 ksi	Y_C=36.7 ksi
S = 15.5 ksi	G_{IC}=0.5 lbf/in
G_{IIC}=0.5 lbf/in	

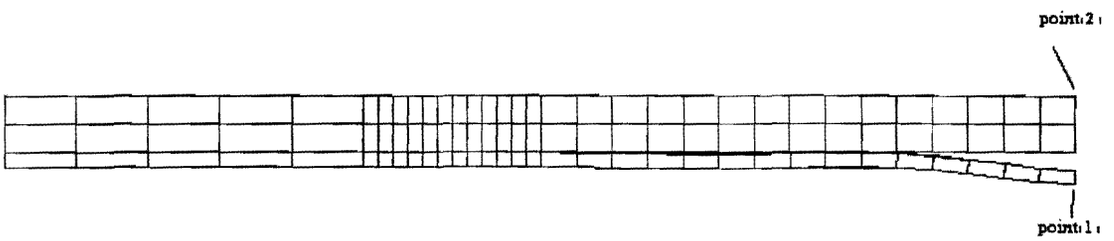

Fig.11: Local buckling

Fig.12: Commencing of global buckling

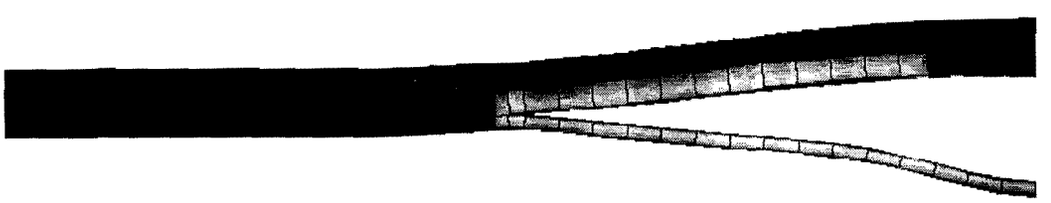

Fig.13: Final global buckling

Fig.14: Load-Disp. Diagram: point(1)

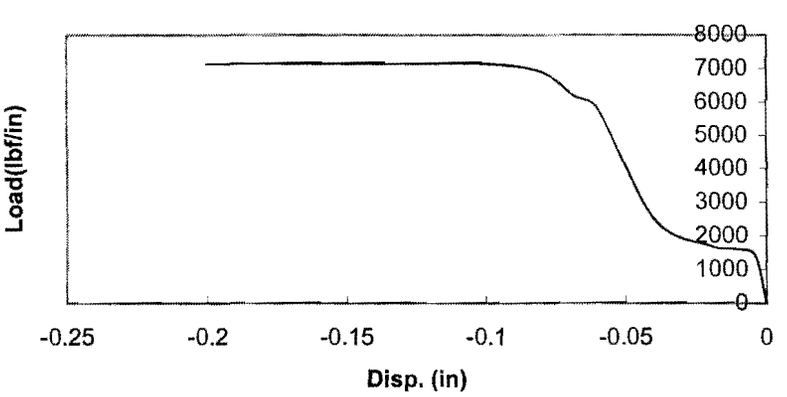

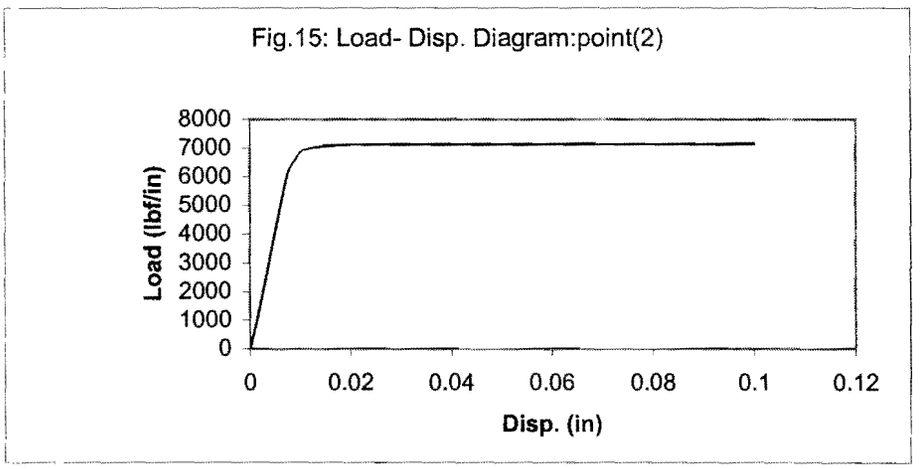

4.3 Delamination and Fracture Analysis of Composite Bend

A fracture analysis has been performed on a 120-degree [0_n/ 90_n/ 0_n] composite bend subjected to downward concentrated loading on its top end. Each laminate is composed of Fiberite T300/1034-C graphite epoxy unidirectional tape. The material properties used in the calculations are listed in Table (3).

Figure 16 depicts the fracture patterns of the bend at two different stage of the loading. An eight-layer discrete element model was implemented for modeling the bend. Apart form early local fractures in the vicinity of the applied loading, progressive fracturing commenced near to the clamped edge of the bend and concentrated in the weak mid-layer of the bend [Figure (16-a)]. Fracturing then spread across the thickness of the bend up to final collapse (16-b).

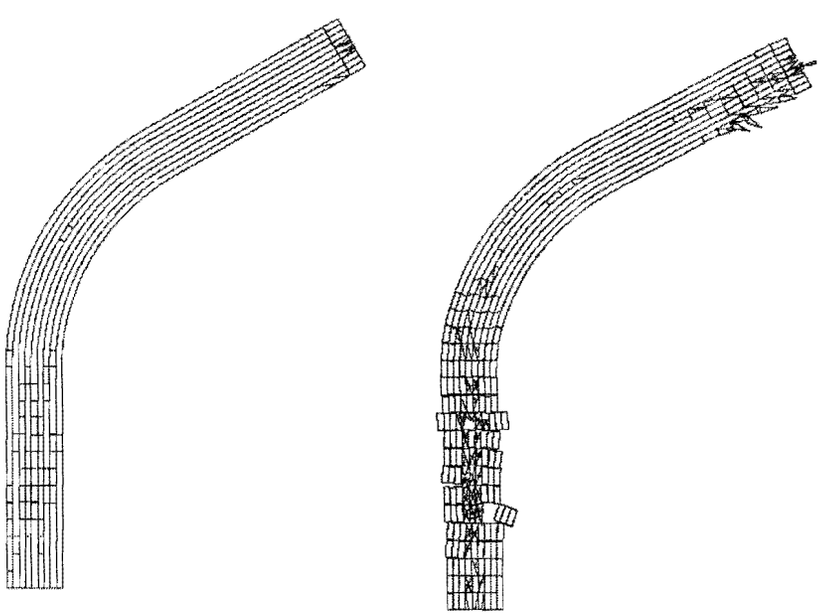

(a) Early fractures (b) Threshold of collapse

Figure 16: Deformamed shape and fracture patterns 0f 120-degree bend subjected to inward loading

Table(3)- Material properties for T300/1034- graphite epoxy	
E_{xx}= 146800 MPa	E_{yy}=11400 MPa
G_{yz}=4380 MPa	G_{xy}=6184 MPa
ν_{yz}=0.3	ν_{xy}=0.3
X_T=1730 MPa	X_C=1380 MPa
Y_T=66.5 MPa	Y_C=26.8 MPa
S = 133.7 MPa	ρ= 1.55 mg/m^3

5. Conclusion

A combined FE/DE element method has been successfully developed for simulation of composites. The algorithm comprises various contact detection and contact interaction schemes to construct a reliable tool for the modeling of complex post failure phenomena. In addition to considering the potential pre-delamination contacts, it also takes into account the contact and friction interactions for post debonding or fracture behaviour of composites. Numerical simulations have shown acceptable results, which can not be achieved by other continuum based methods. These methods are not capable of simulating fragmentation phenomenon or even progressive multi fracturing. Implementing interface elements requires matching nodes on adjacent surfaces, which is not appropriate in a multi crack analysis. Also considering interaction between matrix cracking and delamination can not be easily implemented with other classical methods. Being numerically expensive and requiring complex programming, are among the disadvantages of the proposed scheme. However, it provides a numerical tool for simulations that other techniques are unable to perform.

6. Acknowledgement

The authors would like to acknowledge the support received from the chancellor for research, University of Tehran and the Aircraft Manufacturing Corporation, HESA, Isfahan, Iran.

7. Reference

[1] A. P. Parker, The Mechanics of Fracture and Fatigue, An Introduction, E. & F.N. SPON Ltd, pp. 89-122, 1981.
[2] P. Conti, A.D. Paulis, A Simple Model to Simulate the interlaminar stresses generated near the free edge of a composite laminate, Delamination and Debonding of Materials, ASTM STP 876,pp. 33-51, 1985.
[3] N.J. Pagano (Ed.), Interlaminar Response of Composite Materials, Elsevier, pp. 1-66, 111-159, 1989.
[4] S. Liu, Z. Kutlu, F.K. Chang, Matrix cracking-induced delamination propagation in graphite/epoxy laminated composites due to a transverse concentrate load, Composite Materials: Fatigue and Fracture, ASTM STP 1156,vl. 4, ASTM, pp. 86-101, 1993.
[5] S. Mohammadi, D.R.J. Owen, Peric, "3D Progressive Damage Analysis of Composites by Combined Finite/Discrete Element Approach", ECCOMAS 2000, Barcelona, 11-14 September 2000.
[6] Y.S. Roh and F.K. Chang, "Effect of Impact Damage on Lamb Wave Propagation in Laminated Composites". Dynamic Response and Behaviour of Composites, ASME AD-Vol. 46,pp. 127-138,1995.
[7] Y. MI, M.A. Crisfield and G.A.O. Davies, "Progressive Delamination Using Interface Elements", Journal of Composite Materials, Vol. 32, No. 14,pp. 1246-1269, 1998.
[8] Z. Hashin, "Failure Criteria For Unidirectional Fiber Composites", Journal of Applied Mechanics, Vol. 47, pp. 329-334, 1980.
[9] S. Mohammadi, D.R.J. Owen, Peric, "A Combined Finite/Discrete Element Algorithm for Delamination Analysis of Composites", Finite Element in Analysis and Design, Vol. 28, pp. 321-336, 1998.
[10] S. Mohammadi, S. Foruzansepehr and A. Asadollahi, "A Contact Based Fracture Analysis of Composites", Journal of Thin-Walled Structures, 2002, In Press.
[11] P. H. Geubelle, J. S. Baylor, "Impact-Induced Delamination of Composites", Composites: Part B, 591-615,1998.
[12] P. Progini, A. Riccio, F. Scaramuzzino, "Influence of Delamination Growth and Contact Phenomena on the Compressive Behavior of Composite Panels", Journal of Composite Materials, Vol.33, No. 15, pp.1433-1465, 1999.